Published OnlineFirst May 11, 2011; DOI: 10.1158/1078-0432.CCR-11-0395

Human Cancer Biology

Clinical Cancer Research

Primary Central Nervous System Lymphomas: A Validation Study of Array-Based Comparative Genomic Hybridization in Formalin-Fixed Paraffin-Embedded Tumor Specimens

Esteban Braggio[1], Ellen Remstein McPhail[2], William Macon[2], M. Beatriz Lopes[3], David Schiff[4], Mark Law[2], Stephanie Fink[2], Debra Sprau[2], Caterina Giannini[2], Ahmet Dogan[2], Rafael Fonseca[1], and Brian Patrick O'Neill[2]

Abstract

Purpose: Only a limited number of genetic studies have been conducted in primary central nervous system lymphomas (PCNSL), partly due to the rarity of the tumors and the very limited amount of available tissue. In this report, we present the first molecular characterization of copy number abnormalities (CNA) of newly diagnosed PCNSL by array-based comparative genomic hybridization (aCGH) in formalin-fixed paraffin-embedded (FFPE) specimens and compare the results with matched, frozen tumor specimens.

Experimental Design: We conducted aCGH in FFPE tissues from PCNSL. Results were compared with matched, paired, frozen tumors.

Results: Our analysis confirmed the good to fair quality and reliability of the data generated from limited amounts of tumoral FFPE tissue. Overall, all PCNSL cases were characterized by highly complex karyotypes, with a median of 23 CNAs per patient (range, 17–47). Overall, 20 chromosomal regions were recurrently found in more than 40% of cases. Deletions of 6p21, 6q, and 9p21.3 and gain of 12q12-q24.33 were the commonest CNAs. Other minimal affected regions were defined, and novel recurrent CNAs affecting single genes were identified in 3q26.32 (*TBL1XR1*) and 8q12.1 (*TOX*).

Conclusions: The results obtained are encouraging. Larger archival tissue collections can now be analyzed to complement the still fragmented knowledge we have of the genetic basis of the PCNSL. *Clin Cancer Res; 17(13); 4245–53. ©2011 AACR.*

Introduction

Primary central nervous system lymphoma (PCNSL) is an aggressive primary brain tumor characterized by a perivascular accumulation of malignant cells that have lymphoid characteristics. Its cell of origin and tumorigenesis are unknown. PCNSL is typically lethal without treatment, is increasing in incidence, and targets vulnerable populations (1, 2). It is therapy responsive, and its aggressive management may lead to remission (3, 4). However, current treatments are not increasing cure rates (5) and the quality of such survival is often poor (6, 7). PCNSL has a disproportionate effect on quality of life because of its disabling impact on cognition, language, mobility, and adaptive skills. The advanced age of the average patient and neurotoxicity of standard therapy further amplify this morbidity.

The 2000 NCI-NINDS PRG report stated that "Molecular characterization of PCNSL tumorigenesis is now needed to inform pathogenesis-based treatment and prevention strategies" (8). To that end, a series of gene function–oriented publications including our own have identified chromosomal abnormalities that may have pathogenetic relevance (9). For example, deletions of 6q are a frequent observation in systemic diffuse large B-cell lymphoma (DLBCL) and are typically associated with a worse prognosis (10, 11). Cady and colleagues described a similar association of 6q22–23 deletions and prognosis in PCNSL patients with no apparent immunodeficiency and stated that the deletion implied a loss or modification of a tumor suppressor gene, *PTPRK* (11). In contrast, posttransplant lymphoproliferative disorder of the central nervous system (CNS), the Epstein–Barr virus (EBV)-driven PCNSL-like disease seen in organ transplant recipients and other immunosuppressed states, is not associated with deletions of 6q or abnormalities of *c-MYC* and *BCL-6*, suggesting a distinct pathogenesis (12).

Unlike systemic DLBCL and other forms of non–Hodgkin's lymphomas, relatively little is known about the biology of PCNSL. Only a limited number of genetic

Authors' Affiliations: [1]Department of Biochemistry, Mayo Clinic, Scottsdale, Arizona; [2]Department of Neurology, Mayo Clinic, Rochester, Minnesota; and Departments of [3]Pathology and [4]Neurology, University of Virginia, Charlottesville, Virginia

Note: Supplementary data for this article are available at Clinical Cancer Research Online (http://clincancerres.aacrjournals.org/).

The *Mayo SPORE in Brain Cancer* (B.P. O'Neill and C. Giannini) and *the Iowa/Mayo Lymphoma SPORE* (E.R. McPhail, W. Macon, and A. Dogan).

Corresponding Author: Brian Patrick O'Neill, Department of Neurology, Mayo Clinic, 200 SW First Street, Rochester, MN 55905. Phone: 507-266-4126; Fax: 507-538-6012; E-mail: boneill@mayo.edu

doi: 10.1158/1078-0432.CCR-11-0395

Published OnlineFirst May 11, 2011; DOI: 10.1158/1078-0432.CCR-11-0395

Translational Relevance

Genomic analysis has been challenging in primary central nervous system lymphomas (PCNSL), mainly due to the rarity of the tumors and the very limited amount of available tissue. In this study, we used tissue extracted from formalin-fixed paraffin-embedded (FFPE) blocks to conduct array-based comparative genomic hybridization (aCGH) assays in PCNSL. The good quality of the results is encouraging. Larger archival tissue collections can now be analyzed to complement the still fragmented knowledge we have of the genetic basis of PCNSL, which is based on a very few studies conducted in small cohorts. In addition, we used an aCGH platform that provided us with the highest resolution analysis of the PCNSL genome conducted to date and it enabled us to identify novel recurrent abnormalities affecting potential key genes in PCNSL pathogenesis.

studies have been conducted, partly due to the rarity of the tumors (3% of all primary brain tumors; ref. 13) and the very limited amount of available tissue. PCNSL lesions are typically deep-seated and usually best approached by stereotactic techniques (14). Aggressive debulking does not improve prognosis (13, 14), thus limiting the amount of tissue that can be safely removed, and specimens are typically exhausted by the diagnostic workup. In addition, no cell lines have been established in PCNSL, thus making the selection of appropriate *in vitro* systems for genomic validations and functional analysis more difficult. In PCNSL, the source of biological samples is often limited to formalin-fixed and paraffin-embedded (FFPE) specimens. These specimens represent valuable materials for cancer research, especially in retrospective studies with long follow-up data, but its use in systematic studies has been challenging because the yield of DNA obtained from this source is often very degraded. However, in recent years, there has been progress in the use of FFPE specimens for whole-genome array-based studies in solid tumors (15–17).

In this report, we describe the molecular characterization of copy number abnormalities (CNA) by array-based comparative genomic hybridization (aCGH) in matched FFPE and frozen tumor specimens taken from newly diagnosed PCNSL patients without apparent immunodeficiency. The aim of this study was, first, to better characterize the disease at chromosomal and gene levels and to correlate these features with clinical and pathologic features and, second, to validate the use of aCGH in FFPE tumor specimens as an alternative to frozen specimens.

Patients and Methods

Tumor samples

Frozen PCNSL tumor samples in pellets and FFPE blocks were retrieved from the Mayo Clinic Tumor Registry (Mayo Foundation IRB approval 08-001933) and the University of Virginia (University of Virginia IRB approval 14225). A review of clinical histories confirmed that each case was newly diagnosed, was confined to the CNS, and had no occult disease by standard staging and that each patient had no apparent immunodeficiency. Given the limited number of patients and the pilot nature of the study, statistical analyses were not done.

Three 3-μm sections were cut from each pellet and placed on clean glass slides. One slide was stained with hematoxylin–eosin (H&E) to confirm sufficient tumor-rich tissue without significant hemorrhage, necrosis, or artifact. Confirmatory immunohistochemistry (IHC) using antibodies directed against CD20 and CD3 was done on the second and third slides of each patient set. All confirmed cases were then screened for EBV, utilizing *in situ* hybridization probes that recognize EBV-encoded RNA (EBER). Any nuclear staining in tumor cells was viewed as a positive result. The specimens were subgrouped as germinal center (GC) or non-GC by IHC for CD10, MUM-1, and BCL-6, according to the Hans algorithm (18). Immunostaining was done in 1 batch to maximize laboratory efficiency. Each batch contained positive and negative controls and replicates from each case. Lymphomas were considered positive if 30% or more of the cells stained with antibody. Data on the intensity of staining were not used because of potential variations in tissue fixation and processing.

DNA isolation

Genomic DNA was obtained from frozen tumors by using the Puregene Core A Kit (Qiagen) according to manufacturer's recommendations. In the FFPE specimens, a slide was cut and stained as aforementioned to confirm the richness of tumors. In cases for which tumor burden was less than 70%, tumor areas were identified on the H&E-stained section. These areas were macrodissected to minimize normal tissue content. Samples were deparaffinized using heptane at room temperature for 1 hour. Methanol was added and the sample was pelleted by centrifugation. DNA was obtained using the AllPrep DNA/RNA FFPE Kit (Qiagen) according to manufacturer's recommendations. DNA concentration and purity were measured by spectrophotometry, and DNA integrity was assessed on a 1% agarose gel.

Array-based comparative genomic hybridization

To assess the reliability of FFPE samples, we conducted a comparison of assay performance between snap-frozen and FFPE samples in 6 PCNSL specimens. In an additional case, only the frozen tumor sample was analyzed.

Snap-frozen samples

aCGH was done in 3 samples with the Human Genome 244A microarray and in the remaining 4 with the Human Sureprint G3 microarray (Agilent Technologies). The digestion, labeling, and hybridization steps were done as previously described (19). Microarrays were scanned in a DNA Microarray scanner (Agilent Technologies). Feature

Published OnlineFirst May 11, 2011; DOI: 10.1158/1078-0432.CCR-11-0395

extraction was done with Feature Extraction Software (version 9.5; Agilent Technologies). Extracted data were imported and analyzed using Genomic Workbench (version 5.0.14; Agilent Technologies) and Nexus 5.1 (Biodiscovery).

FFPE samples

aCGH was done on 6 FFPE specimens, using the Human Genome 244A microarray. Briefly, 2 μg of reference DNA was fragmented by heating at 95°C for 10 minutes. Fragmentation was not necessary for the FFPE samples. Samples were labeled with the ULS kit (Agilent) for FFPE tissues according to manufacturer's recommendation. Labeled genomic reactions were cleaned up with KREApure columns (Agilent Technologies) and hybridized at 65°C for 40 hours. Scanning and data analysis were the same as those for the snap-frozen samples.

Data analysis

Copy number abnormalities (CNAs) were calculated using aberration detection module 1 and RANK segmentation algorithms in Genomic Workbench and Nexus software, respectively (20). The derivative of the log ratio spread (DLRSpread) across the entire genome was calculated and used as a surrogate of assay quality. Assays with DLRSpread values lower than 0.2 are considered excellent; values between 0.2 and 0.3 are considered good; and values higher than 0.3 are considered marginal. Both a 2-probe filter (0.25_log_2; 244K array format) and a 3-probe filter (0.25_log_2; Sureprint G3 format) were used in the aberration detection of fresh samples, obtaining an average genomic resolution of 17 and 4.5 kb, respectively. Copy number variations were identified and excluded from the analysis as previously described (19).

FISH

Interphase FISH for 6q22 and 9p21 loci was done using custom DNA probes as previously reported (11) or, if one existed, a commercially available probe was used according to the manufacturer's instructions. A minimum of 50 tumor cells were scored. A cohesive group of at least 20 cells, of which at least 80% were abnormal, was required for the sample to be considered abnormal.

Results

Clinical characteristics

The cohort comprised 7 patients, 2 men and 5 women, with median age of 60 years (range, 52–77 years). All cases were histologically reconfirmed as CD20-positive DLBCL. Each specimen had diagnostic tissue without hemorrhage or necrosis; and each specimen was EBER negative. Three patients were identified at Mayo Clinic and 4 at the University of Virginia. No patient was HIV positive, had received a solid organ transplant, or had an active autoimmune disorder. Clinical details are shown in Table 1. Performance score could be ascertained in 5 patients. Survival data were available for all 7 patients (cases A–G) and treatment information for 5 patients (cases A–D and G). Treatment varied from patient to patient. Median survival of the 5 treated patients was 12 months. Two patients received no treatment and survived 2.5 months and 3 weeks, respectively (cases B and D).

Of the 7 PCNSL patients, 3 were classified as having a GC phenotype and the remaining 4 as non-GC phenotype (ABC). In 6 of these 7 PCNSL patients (cases B–G), aCGH experiments were conducted on DNA samples obtained from both snap-frozen and FFPE tissues for assay quality comparative purposes. In the remaining sample (case A), only frozen sample was analyzed.

Performance of aCGH experiments in samples from FFPE and snap-frozen specimens

To measure the assay quality of the aCGH experiments, we used the DLRSpread value as a surrogate of signal noise. All aCGH experiments run on snap-frozen tumor specimens showed DLRSpread values in the range of good or excellent, based on QC thresholds obtained from Genomic

Table 1. Clinical characteristics of the patients included in this study

	Case A	Case B	Case C	Case D	Case E	Case F	Case G
Gender	F	M	F	F	F	M	F
Age at diagnosis	63	77	52	59	69	60	54
PS	1	N/A	N/A	3	2	2	2
Pathology	DLBC	DLBC	DLBC	DLBC	DLBC	DLBC	DLBC
Subtype	GC	GC	GC	Non-GC	Non-GC	Non-GC	Non-GC
Treatment	CHOD-BLEO + RT	None	HDMTX	None	N/A[a]	N/A[a]	R-MPV
Survival (mo)	105	2.5	8+ (alive)	<1	10	12	26+ (alive)

Abbreviations: PS, performance status; CHOD-BLEO, cyclophosphamide, vincristine, adriamycin, dexamethasone, and bleomycin; RT, radiotherapy; HDMTX, high-dose methotrexate; R-MPV, rituximab, methotrexate, procarbazine, and vincristine; N/A, not available.

[a]Patients treated but details not known.

Published OnlineFirst May 11, 2011; DOI: 10.1158/1078-0432.CCR-11-0395

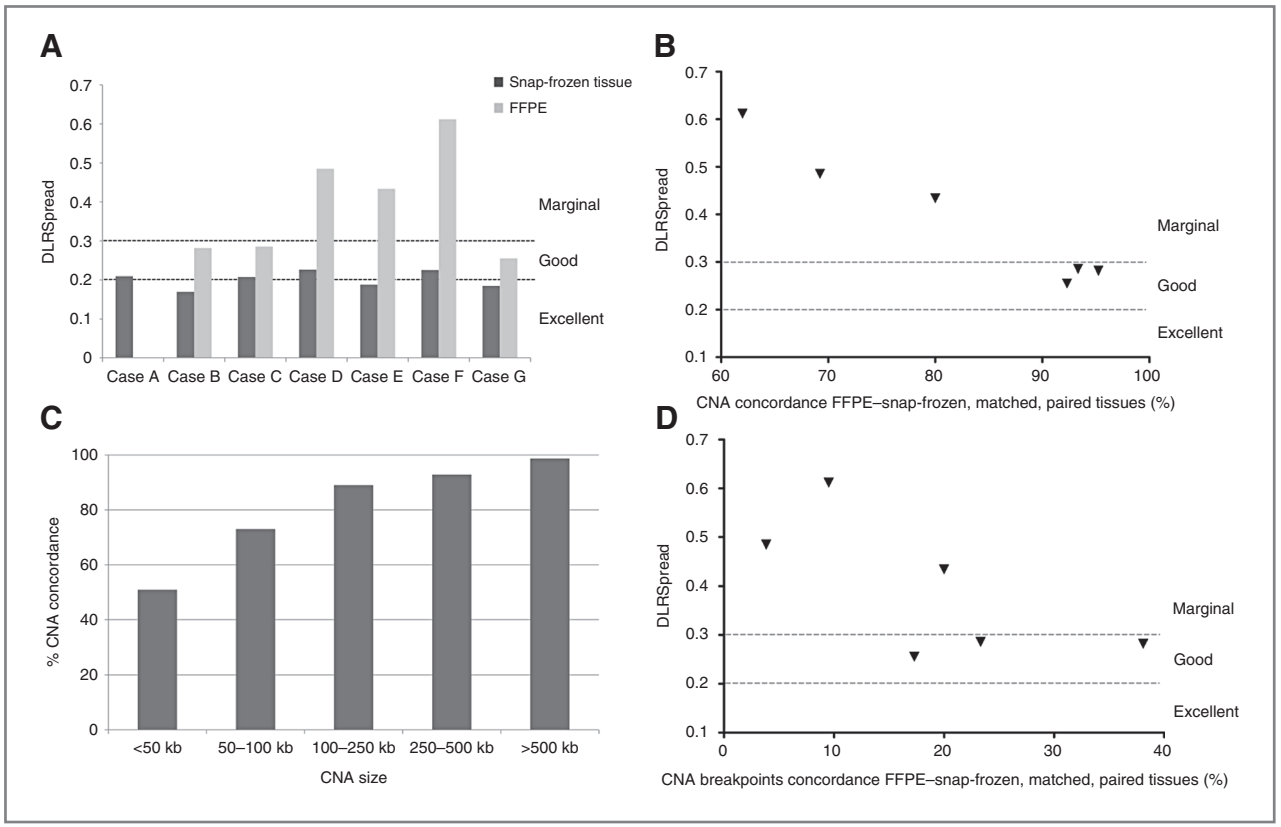

Figure 1. A, assay quality comparison between matched paired FFPE and snap-frozen samples. Case A was analyzed only from snap-frozen sample. B, correlation between assay quality (DLRSpread used as a surrogate) and the CNA concordance level between matched paired FFPE and snap-frozen samples. DLRSpread values below 0.2 correspond to excellent quality assays; values between 0.2 and 0.3 correspond to good quality; and values above 0.3 are considered marginal. C, the concordance of CNA detection between paired samples increases with the size of the abnormalities; D, graph showing that higher-quality assay is associated with higher concordance of CNA breakpoint location between paired samples.

Workbench software. On the other hand, experiments run on FFPE tumor specimens showed higher DLRSpread than paired frozen samples, with 3 assays considered in the good range and another 3 in the marginal range (Fig. 1A).

Next, we analyzed the reliability of the CNA detection in assays run on FFPE specimens compared with the paired frozen samples. The data showed an inverse correlation between DLRSpread values and the concordance of aberration calls between pairs of samples (Fig. 1B). In FFPE cases with low DLRSpread values (<0.3), there was an excellent equivalence in aberration calls, with nearly identical results for frozen samples (92.3%–95.2%). The FFPE cases with higher DRLSpread values (>0.3) showed lower but still significant equivalence, with values ranging from 62% to 80%. Discrepancies in the aberration calls were mainly observed in CNAs smaller than 50 kb (50%) but became very infrequent in CNAs larger than 100 kb (Fig. 1C).

Finally, the main limitation associated with the use of FFPE specimens was the inability to identify the precise location of the CNA breakpoints, with low concordance values ranging from 17.1% to 38.1% in assays with good DLRSpread values and from 3.8% to 20% in poor quality assays (Fig. 1D).

Characterization of CNA in PCNSL

All PCNSL cases were characterized by highly complex genomes, with a median of 23 CNAs per patient (total of 210 CNAs; range, 17–47). Deletions were more common than gains, comprising almost 70% of the CNAs (61.5% of monoallelic and 7.1% of biallelic deletions). The remaining 30% were 1 copy gain, with the exception of 1 CNA characterized by the acquisition of 2 extra copies.

Overall, 20 chromosomal regions were recurrently affected in 3 or more cases, 9 of those being copy number losses and the remaining 11 comprising copy number gains. Deletion of 9p21.3 and gain of 12q12-q24.33 were the most common CNAs, observed in 5 of 7 cases each (Fig. 2 and Table 2), as previously found in other reports (21, 22). The minimal deleted region (MDR) at 9p21.3 targets the *CDKN2A* locus, being biallelically affected in 2 of 5 cases. These deletions were further confirmed using FISH. The minimal amplified region (MAR) on chromosome 12 includes almost the whole q arm (95.2 Mb). Chromosome arms 6p and 6q were also deleted in 5 cases each, but there was not a unique deleted region common to all cases. In 6p arm, several CNAs were found in cytoband 6p21 affecting *HLA* genes and in 2 cases the deletion was

Published OnlineFirst May 11, 2011; DOI: 10.1158/1078-0432.CCR-11-0395

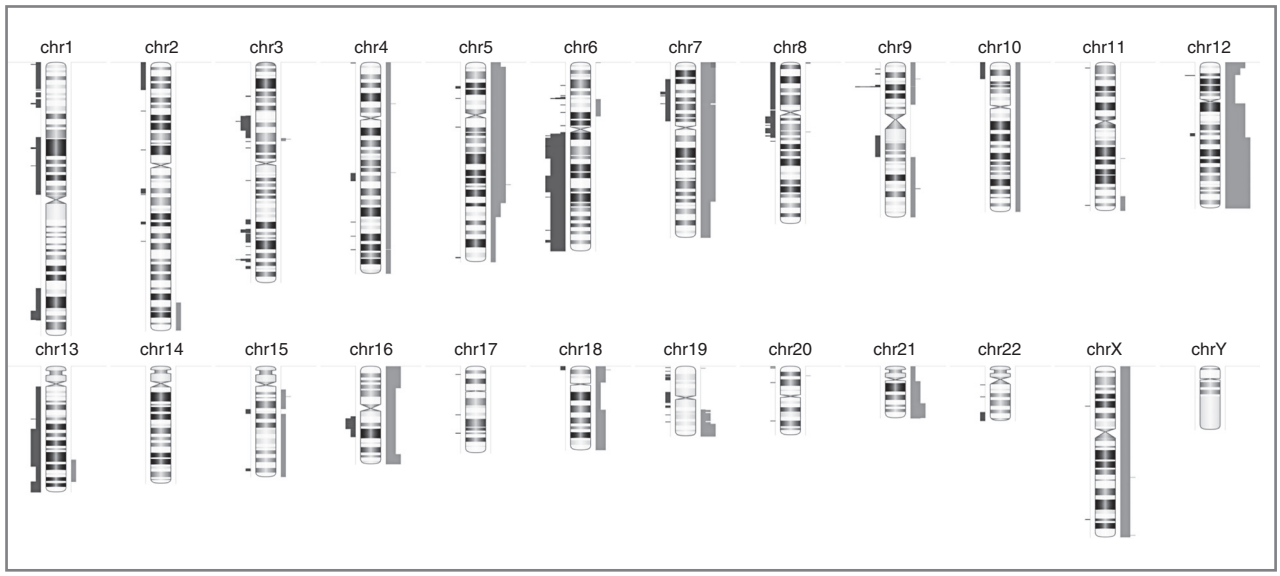

Figure 2. Overview of CNAs identified in this study. Bars at the left of the chromosomes represent losses, and bars at the right represent gains. The amplitude of the bars denotes the frequency within which each region was affected.

biallelic. In cases with 6q deletions, cytobands q12-q14.3, q16.3-q22.2, q22.31, and 6q25.1 were lost in 4 of 5 cases each (Fig. 3). *PTPRK*, previously analyzed by Cady and colleagues (11), was found deleted only in 3 patients by aCGH.

Other frequent alterations were gains of 5p15.33-q23.3, 7p14.2-p22.3, 12p13.31, 16p12.3-p13.3, 18p11.31, 19q13.43, 21q22.11-q22.3, Xq22.1, and Xq28 and losses of 3p21.1 and 3q26.32 (Table 2). On cytoband 3q26.32, a recurrent focal deletion, was found in 3 cases encompassing one gene, the transducin (beta)-like 1 X-linked receptor 1 (*TBL1XR1*).

A total of 15 regions were biallelically deleted, affecting 18 genes (Table 3). Besides the aforementioned losses on 6p21 and 9p21, a recurrent biallelic deletion was found in 6q14.1, including the sole gene *TMEM30A*. Other genes of interest targeted by biallelic deletions were thymocyte selection-associated high-mobility group box (*TOX*) and the *ETV6* (*TEL*) on 8q12.1 and 12p13, respectively. On the other hand, 2 extra copies of 7p22.1-p22.3 were found in 1 case, targeting *CARD11* and another 42 genes (Table 3).

Finally, 144 genes were located in chromosomal breakpoints (Supplementary Table S1). Several of these genes, such as *ETV6*, *NCOA2*, and *FOXP1*, were previously identified as being part of fusion protein in other hematologic diseases.

Discussion

In PCNSL, the source of biological samples is often limited to FFPE specimens. Only recently, aCGH has become a feasible methodology to be used in FFPE specimens (15–17). In this study, we present the first data obtained from FFPE specimens of PCNSL cases. Our analysis confirmed the good to fair quality and reliability of the data generated from a very limited amount of FFPE tissue. The results have encouraged us to analyze larger archival tissue collections to complement the still fragmented knowledge we have of the genetics basis of PCNSL.

On the basis of our earlier observation that deletion of chromosomal region 6q22-23 by FISH correlated with shorter survival of PCNSL patients (14), one of the main goals of this study was to study this chromosomal region of interest in more detail by aCGH. Early studies in PCNSL showed loss of 1 or 2 copies of 6q22-23 in 66% of cases in a small series (23). More precise mapping implicated the *PTPRK* gene within the 140 kb common minimally deleted region in these cases, and deletion of this region was often associated with loss of expression of *PTPRK*. Furthermore, this small series also showed that LOH at the *PTPRK* locus, as well as lack of PTPRK protein expression, was associated with a poorer prognosis (24). Of note, 6q22 was only deleted in 3 of 5 cases with 6q losses. Our aCGH findings are in agreement with previous studies in DLBCL and other B-cell malignancies showing multiple affected regions on 6q without a unique MDR to all cases (25, 26).

Previous comprehensive copy number analysis in PCNSL was done with spatial resolutions ranging from 200 kb to several megabases (21, 22, 27). In this study, we improved the resolution of the analysis, reaching an average of 6 and 17 kb by using Agilent G3 and 244A platforms, respectively. As a result, we were able to refine previously identified MDR/MAR and identify several novel abnormalities affecting tumor suppressor genes and oncogenes potentially implicated in the pathogenesis of PCNSL.

Published OnlineFirst May 11, 2011; DOI: 10.1158/1078-0432.CCR-11-0395

Table 2. Summary of the most commonly involved regions in CNA

Chromosome region	Cytoband	Length (Mb)	Event	%	Genes, *n*	Gene symbols
chr3: 53, 188, 281–53, 220, 792	p21.1	0.03	Loss	42.86	1	*PRKCD*
chr3: 178, 243, 320–178, 531, 406	q26.32	0.29	Loss	42.86	1	*TBL1XR1*
chr5: 4, 025, 353–127, 435, 612	p15.33–q23.3	123.41	Gain	42.86	460	
chr6: 32, 560, 987–32, 591, 889	p21.32	0.03	Loss	57.14	3	*HLA-DRA*, *HLA-DRB1*, *HLA-DRB5*
chr6: 68, 245, 865–87, 035, 064	q12–q14.3	18.79	Loss	57.14	64	
chr6: 102, 568, 948–117, 578, 748	q16.3–q22.2	15.01	Loss	57.14	79	
chr6: 121, 651, 884–121, 998, 751	q22.31	0.35	Loss	57.14	2	*c6orf170*, *GJA1*
chr6: 151, 726, 681–152, 128, 179	q25.1	0.4	Loss	57.14	5	*ZBTB2*, *RMND1*, *c6orf211*, *c6orf97*, *ESR1*
chr6: 160, 706, 067–163, 042, 970	q25.3–q26	2.34	Loss	57.14	8	*SLC22A3*, *LPAL2*, *LPA*, *PLG*, *MAP3K4*, *MTK1*, *AGPAT4*, *PARK2*
chr7: 0–37, 224, 176	p22.3–p14.2	37.22	Gain	42.86	230	
chr9: 21, 952, 671–21, 976, 825	p21.3	0.02	Loss	71.43	1	*CDKN2A*
chr12: 0–5, 440, 239	p13.33–p13.31	5.44	Gain	57.14	47	
chr12: 37, 153, 346–132, 349, 534	q12–q24.33	95.2	Gain	71.43	796	
chr16: 0–19, 949, 848	p13.3–p12.3	19.95	Gain	42.86	312	
chr16: 79, 529, 380–88, 827, 254	q23.2–q24.3	9.3	Gain	42.86	109	
chr18: 3, 006, 092–3, 586, 303	p11.31	0.58	Gain	42.86	5	*MYOM1*, *MRCL3*, *MRLC2*, *TGIF1*, *DLGAP1*
chr19: 52, 173, 665–63, 811, 651	q13.32–q13.43	11.64	Gain	42.86	618	
chr21: 33, 423, 626–46, 862, 008	q22.11–q22.3	13.44	Gain	42.86	159	
chrX: 100, 348, 062–100, 668, 066	q22.1	0.32	Gain	42.86	8	*DRP2*, *TAF7L*, *TIMM8A*, *BTK*, *RPL36A*, *GLA*, *HNRNPHA2*, *ARMCX4*
chrX: 152, 713, 724–152, 889, 525	q28	0.18	Gain	42.86	9	*SSR4*, *PDZD4*, *L1CAM*, *LCAP*, *AVPR2*, *ARHGAP4*, *ARD1A*, *RENBP*, *HCFC1*

NOTE: In all regions smaller than 5 Mb, the genes included are summarized.

Published OnlineFirst May 11, 2011; DOI: 10.1158/1078-0432.CCR-11-0395

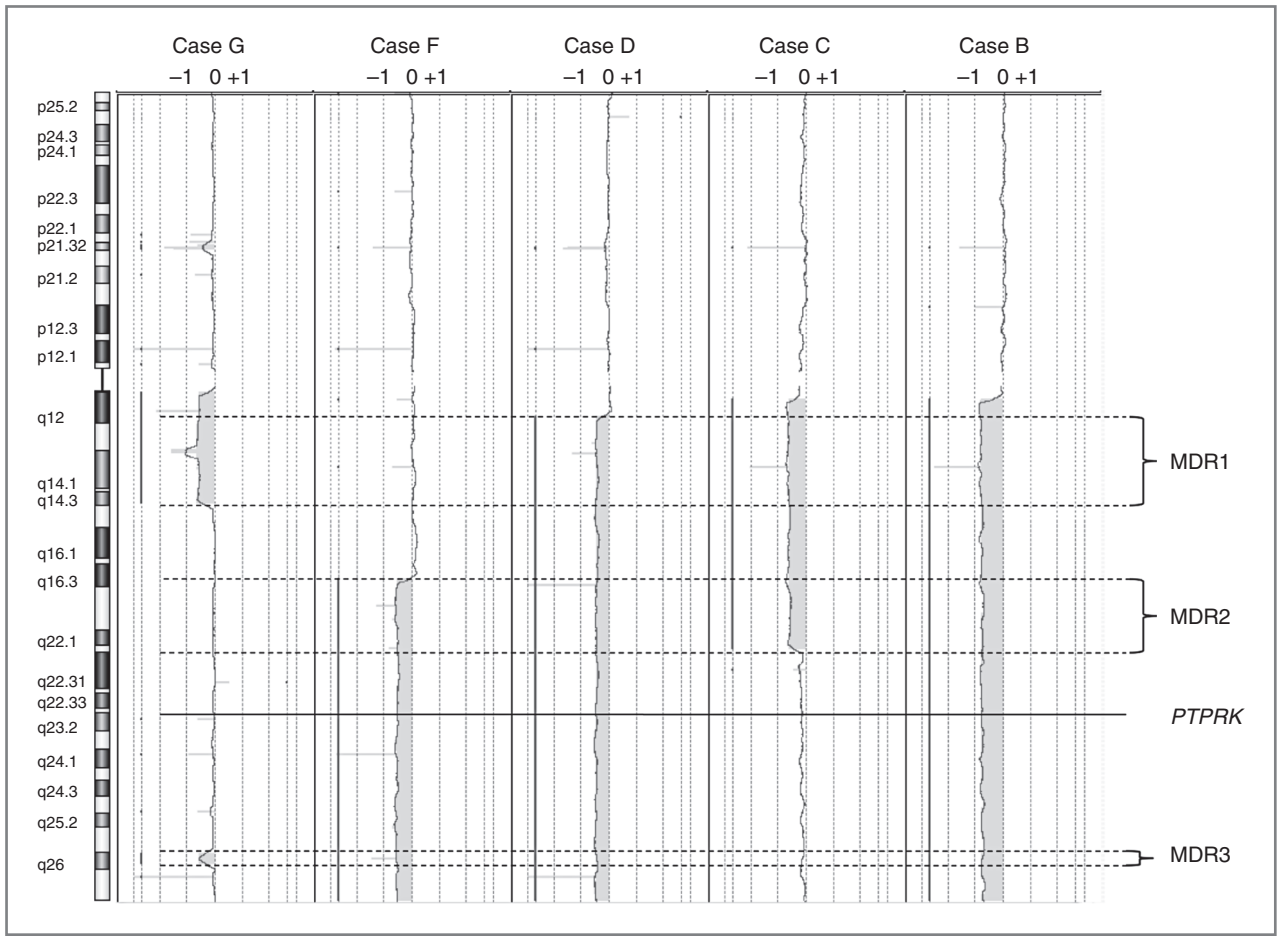

Figure 3. Overview of 6q status. The 3 most commonly deleted regions (MDR1–MDR3) are highlighted. None of them includes *PTPRK* (solid line).

Although including few cases, our preliminary analysis identified potential hits to be followed in larger analysis. Genetic and epigenetic alterations affecting *CDKN2A* (9p21.3) have been previously identified in PCNSL (21, 22, 28). Here we found CNA in 5 of 7 cases, with biallelic deletions observed in 2 cases. The resolution of the approach used provides a better appreciation of the precise prevalence of abnormalities affecting this and other critical genes.

A recurrent focal deletion was found on 3q26.32 targeting exclusively *TBL1XR1*. This gene is a transcriptional regulator that interacts with the corepressors of nuclear hormone receptor (NHR; ref. 29). Monoallelic deletions and the significant associated underexpression of *TBL1XR1* have been recently reported in 12% to 15% of *ETV6-RUNX1*–positive acute lymphoblastic leukemias (30, 31). It has been hypothesized that loss of *TBL1XR1* would compromise the ability of corepressor complexes to inhibit receptor activity, leading to the activation of receptor target genes in the presence of *TBL1XR1* deletions (31). In fact, experiments on knocking down the expression of *TBL1XR1* have removed the capacity of retinoic acid to induce gene expression (32). Of interest, *TBL1XR1* is widely expressed in hematopoietic tissues and may have a key regulatory role in the nuclear factor κB (NF-κB) pathway (32) and Wnt-mediated transcription (33), thus suggesting its potential biological role in PCNSL pathogenesis.

Recurrent loss of 8q12.1, including biallelic loss in 1 case, has allowed us to refine previously described MDR (22) and to identify *TOX* as the target gene. *TOX* has been associated with CD4 T-lineage development (34). Furthermore, a reduction of the spleen IgG B-cell population in a *TOX*-deficient mouse may be suggestive of the TOX involvement in the B-cell differentiation arrest (34).

Additional focal monoallelic deletions affecting negative regulators of the NF-κB signaling pathway (*MAP4K1*, *TANK*, *TAX1BP1*, *TRIB3*) and cell-cycle (*RB1*), and immune-cell regulation (*SIRPB1*, *CBLB*, *NFATC2*) were also identified. Further analyses are needed to study in more detail these genes and their potential involvement in PCNSL pathogenesis.

In summary, the study reported here expanded the spectrum of chromosomal regions of interest, identified several highly prevalent regions that are thought to be biologically important, and showed that FFPE-based aCGH was feasible and reliable in PCNSL cases, thus expanding

Published OnlineFirst May 11, 2011; DOI: 10.1158/1078-0432.CCR-11-0395

Table 3. Summary of homozygous deletions and high copy gains found in this study

Chromosome region	Cytoband	Event	Cases, *n* (%)	Genes, *n*	Gene symbols
chr1: 116, 859, 354-117, 100, 041	p13.1	HD	1 (14)	4	*CD2*, *CD58*, *IGSF3*, *MIR320B1*
chr6: 32, 629, 163-32, 634, 358	p21.32	HD	1 (14)	1	*HLA-DRB6*
chr6: 32, 714, 838-32, 729, 809	p21.32	HD	1 (14)	1	*HLA-DQA1*
chr6: 76, 012, 417-76, 024, 847	q14.1	HD	2 (29)	1	*TMEM30A*
chr6: 108, 336, 870-108, 343, 503	q21	HD	1 (14)	1	*SEC63*
chr7: 30, 093, 598-30, 097, 504	p15.1	HD	1 (14)	1	*PLEKHA8*
chr8: 59, 992, 790-60, 127, 684	q12.1	HD	1 (14)	1	*TOX*
chr9: 21, 945, 445-22, 005, 131	p21.3	HD	2 (29)	4	*CDKN2A*
chr12: 11, 782, 161-12, 006, 002	p13.2	HD	1 (14)	1	*ETV6*
chr16: 51, 779, 820-51, 925, 504	q12.2	HD	1 (14)	1	*CHD9*
chr17: 60, 450, 022-60, 483, 624	q24.1	HD	1 (14)	1	*GNA13*
chrX: 75, 688, 281-76, 338, 275	q13.3–q21.1	HD	1 (14)	1	*MIR384*
chrX: 138, 465, 809-138, 748, 476	q27.1	HD	1 (14)	3	*ATP11C*, *F9*, *MCF2*
chr7: 0-4, 951, 238	p22.3–p22.1	High copy gain	1 (14)	43	*ADAP1*, *AMZ1*, *C7orf27*, *C7orf50*, *CARD11*, *CHST12*, *COX19*, *CYP2W1*, *EIF3B*, *ELFN1*, *FAM20C*, *FLJ44511*, *FOXK1*, *FTSJ2*, *GET4*, *GNA12*, *GPER*, *GPR146*, *HEATR2*, *INTS1*, *IQCE*, *KIAA0415*, *KIAA1908*, *LFNG*, *MAD1L1*, *MAFK*, *MICALL2*, *MIR339*, *MMD2*, *NUDT1*, *PAPOLB*, *PDGFA*, *PRKAR1B*, *PSMG3*, *RADIL*, *SDK1*, *SNX8*, *SUN1*, *TFAMP1*, *TMEM184A*, *TTYH3*, *UNCX*, *ZFAND2A*

Abbreviation: HD, homozygous deletions.

the repertoire of investigative tools in this tumor. A better understanding of the underlying mechanisms leading to PCNSL development could result in the identification of prognostic markers and therapeutic targets.

Disclosure of Potential Conflicts of Interest

R. Fonseca received research sponsorship from Cylene, Onyx, and Celgene and a patent for prognostication of MM based on genetic characterization of the disease. R. Fonseca also receives consulting fees from Medtronic, Otsuka, Celgene, Genzyme, BMS, and AMGEN.

Grant Support

The work reported here was supported in part by "Steve's Run"; the Mayo SPORE in Brain Cancer (P50CA108961; PI: B.P. O'Neill), including SPORE Supplement P50CA108961-03S1 (to B.P. O'Neill); and the Iowa/Mayo Clinic Lymphoma SPORE (P50CA97274; PI: G. Weiner).

The costs of publication of this article were defrayed in part by the payment of page charges. This article must therefore be hereby marked *advertisement* in accordance with 18 U.S.C. Section 1734 solely to indicate this fact.

Received February 11, 2011; revised April 27, 2011; accepted May 3, 2011; published OnlineFirst May 11, 2011.

References

1. Ferreri AJ, Reni M. Primary central nervous system lymphoma. Crit Rev Oncol Hematol 2007;63:257–68.
2. Olson JE, Janney CA, Rao RD, Cerhan JR, Kurtin PJ, Schiff D, et al. The continuing increase in the incidence of primary central nervous system non-Hodgkin lymphoma: a surveillance, epidemiology, and end results analysis. Cancer 2002;95:1504–10.
3. Abrey LE, Ben-Porat L, Panageas KS, Yahalom J, Berkey B, Curran W, et al. Primary central nervous system lymphoma: the Memorial Sloan-Kettering Cancer Center prognostic model. J Clin Oncol 2006;24:5711–5.
4. Batchelor T, Loeffler JS. Primary CNS lymphoma. J Clin Oncol 2006;24:1281–8.
5. Panageas KS, Elkin EB, DeAngelis LM, Ben-Porat L, Abrey LE. Trends in survival from primary central nervous system lymphoma, 1975–1999: a population-based analysis. Cancer 2005;104:2466–72.
6. Blay JY, Conroy T, Chevreau C, Thyss A, Quesnel N, Eghbali H, et al. High-dose methotrexate for the treatment of primary cerebral lymphomas: analysis of survival and late neurologic toxicity in a retrospective series. J Clin Oncol 1998;16:864–71.
7. O'Neill BP. Neurocognitive outcomes in primary CNS lymphoma (PCNSL). Neurology 2004;62:532–3.
8. Louis DN, Posner J, Jacobs T, Kaplan R. Report of the Brain Tumor Progress Review Group. NCI-NINDS PRG report. NIH: Bethesda, MD; 2000. NIH Publication No. 01-4902.

Published OnlineFirst May 11, 2011; DOI: 10.1158/1078-0432.CCR-11-0395

9. Flordal Thelander E, Ichimura K, Collins VP, Walsh SH, Barbany G, Hagberg A, et al. Detailed assessment of copy number alterations revealing homozygous deletions in 1p and 13q in mantle cell lymphoma. Leuk Res 2007;31:1219–30.
10. Taborelli M, Tibiletti MG, Martin V, Pozzi B, Bertoni F, Capella C. Chromosome band 6q deletion pattern in malignant lymphomas. Cancer Genet Cytogenet 2006;165:106–13.
11. Cady FM, O'Neill BP, Law ME, Decker PA, Kurtz DM, Giannini C, et al. Del(6)(q22) and BCL6 rearrangements in primary CNS lymphoma are indicators of an aggressive clinical course. J Clin Oncol 2008;26:4814–9.
12. Rinaldi A, Kwee I, Poretti G, Mensah A, Pruneri G, Capello D, et al. Comparative genome-wide profiling of post-transplant lymphoproliferative disorders and diffuse large B-cell lymphomas. Br J Haematol 2006;134:27–36.
13. Gerstner ER, Batchelor TT. Primary central nervous system lymphoma. Arch Neurol 2010;67:291–7.
14. O'Neill BP, Kelly PJ, Earle JD, Scheithauer B, Banks PM. Computer-assisted stereotaxic biopsy for the diagnosis of primary central nervous system lymphoma. Neurology 1987;37:1160–4.
15. Paris PL, Sridharan S, Scheffer A, Tsalenko A, Bruhn L, Collins C. High resolution oligonucleotide CGH using DNA from archived prostate tissue. Prostate 2007;67:1447–55.
16. Hostetter G, Kim SY, Savage S, Gooden GC, Barrett M, Zhang J, et al. Random DNA fragmentation allows detection of single-copy, single-exon alterations of copy number by oligonucleotide array CGH in clinical FFPE samples. Nucleic Acids Res 2010;38:e9.
17. Johnson NA, Hamoudi RA, Ichimura K, Liu L, Pearson DM, Collins VP, et al. Application of array CGH on archival formalin-fixed paraffin-embedded tissues including small numbers of microdissected cells. Lab Invest 2006;86:968–78.
18. Hans CP, Weisenburger DD, Greiner TC, Gascoyne RD, Delabie J, Ott G, et al. Confirmation of the molecular classification of diffuse large B-cell lymphoma by immunohistochemistry using a tissue microarray. Blood 2004;103:275–82.
19. Braggio E, Keats JJ, Leleu X, Van Wier S, Jimenez-Zepeda VH, Valdez R, et al. Identification of copy number abnormalities and inactivating mutations in two negative regulators of nuclear factor-kappaB signaling pathways in Waldenstrom's macroglobulinemia. Cancer Res 2009;69:3579–88.
20. Lipson D, Aumann Y, Ben-Dor A, Linial N, Yakhini Z. Efficient calculation of interval scores for DNA copy number data analysis. J Comput Biol 2006;13:215–28.
21. Booman M, Szuhai K, Rosenwald A, Hartmann E, Kluin-Nelemans H, de Jong D, et al. Genomic alterations and gene expression in primary diffuse large B-cell lymphomas of immune-privileged sites: the importance of apoptosis and immunomodulatory pathways. J Pathol 2008;216:209–17.
22. Schwindt H, Vater I, Kreuz M, Montesinos-Rongen M, Brunn A, Richter J, et al. Chromosomal imbalances and partial uniparental disomies in primary central nervous system lymphoma. Leukemia 2009;23:1875–84.
23. Pasqualucci L, Compagno M, Houldsworth J, Monti S, Grunn A, Nandula SV, et al. Inactivation of the PRDM1/BLIMP1 gene in diffuse large B cell lymphoma. J Exp Med 2006;203:311–7.
24. Nakamura M, Kishi M, Sakaki T, Hashimoto H, Nakase H, Shimada K, et al. Novel tumor suppressor loci on 6q22–23 in primary central nervous system lymphomas. Cancer Res 2003;63:737–41.
25. Thelander EF, Ichimura K, Corcoran M, Barbany G, Nordgren A, Heyman M, et al. Characterization of 6q deletions in mature B cell lymphomas and childhood acute lymphoblastic leukemia. Leuk Lymphoma 2008;49:477–87.
26. Lenz G, Wright GW, Emre NC, Kohlhammer H, Dave SS, Davis RE, et al. Molecular subtypes of diffuse large B-cell lymphoma arise by distinct genetic pathways. Proc Natl Acad Sci U S A 2008;105:13520–5.
27. Sung CO, Kim SC, Karnan S, Karube K, Shin HJ, Nam DH, et al. Genomic profiling combined with gene expression profiling in primary central nervous system lymphoma. Blood 2011;117:1291–300.
28. Richter J, Ammerpohl O, Martin-Subero JI, Montesinos-Rongen M, Bibikova M, Wickham-Garcia E, et al. Array-based DNA methylation profiling of primary lymphomas of the central nervous system. BMC Cancer 2009;9:455.
29. Zhang XM, Chang Q, Zeng L, Gu J, Brown S, Basch RS. TBLR1 regulates the expression of nuclear hormone receptor co-repressors. BMC Cell Biol 2006;7:31.
30. Mullighan CG, Goorha S, Radtke I, Miller CB, Coustan-Smith E, Dalton JD, et al. Genome-wide analysis of genetic alterations in acute lymphoblastic leukaemia. Nature 2007;446:758–64.
31. Parker H, An Q, Barber K, Case M, Davies T, Konn Z, et al. The complex genomic profile of ETV6-RUNX1 positive acute lymphoblastic leukemia highlights a recurrent deletion of TBL1XR1. Genes Chromosomes Cancer 2008;47:1118–25.
32. Perissi V, Aggarwal A, Glass CK, Rose DW, Rosenfeld MG. A corepressor/coactivator exchange complex required for transcriptional activation by nuclear receptors and other regulated transcription factors. Cell 2004;116:511–26.
33. Li J, Wang CY. TBL1-TBLR1 and beta-catenin recruit each other to Wnt target-gene promoter for transcription activation and oncogenesis. Nat Cell Biol 2008;10:160–9.
34. Aliahmad P, Kaye J. Development of all CD4 T lineages requires nuclear factor TOX. J Exp Med 2008;205:245–56.

AACR American Association for Cancer Research

Clinical Cancer Research

Primary Central Nervous System Lymphomas: A Validation Study of Array-Based Comparative Genomic Hybridization in Formalin-Fixed Paraffin-Embedded Tumor Specimens

Esteban Braggio, Ellen Remstein McPhail, William Macon, et al.

Clin Cancer Res 2011;17:4245-4253. Published OnlineFirst May 11, 2011.